Modeling the Influence of the E-Cadherin-β-Catenin Pathway in Cancer Cell Invasion: A Multiscale Approach

Ignacio Ramis-Conde,*† Dirk Drasdo,*‡ Alexander R. A. Anderson,† and Mark A. J. Chaplain†
*French National Institute for Research in Computer Science and Control (INRIA), Domaine de Voluceau-Rocquencourt, Le Chesnay, France; †Division of Mathematics, The University of Dundee, Dundee, Scotland; and ‡Interdisciplinary Centre for Bioinformatics (IZBI), University of Leipzig, Leipzig, Germany

ABSTRACT In this article, we show, using a mathematical multiscale model, how cell adhesion may be regulated by interactions between E-cadherin and β-catenin and how the control of cell adhesion may be related to cell migration, to the epithelial-mesenchymal transition and to invasion in populations of eukaryotic cells. E-cadherin mediates cell-cell adhesion and plays a critical role in the formation and maintenance of junctional contacts between cells. Loss of E-cadherin-mediated adhesion is a key feature of the epithelial-mesenchymal transition. β-catenin is an intracellular protein associated with the actin cytoskeleton of a cell. E-cadherins bind to β-catenin to form a complex which can interact both with neighboring cells to form bonds, and with the cytoskeleton of the cell. When cells detach from one another, β-catenin is released into the cytoplasm, targeted for degradation, and downregulated. In this process there are multiple protein-complexes involved which interact with β-catenin and E-cadherin. Within a mathematical individual-based multiscale model, we are able to explain experimentally observed patterns solely by a variation of cell-cell adhesive interactions. Implications for cell migration and cancer invasion are also discussed.

INTRODUCTION

Cancer is characterized by multiple mutations in a single cell leading to a loss of control in cell replication accompanied by an uncontrolled growth of the total cell mass, eventually leading to the formation of an in situ solid tumor. After the tumor reaches a certain size, genetic instability in the cancer cells may lead to further dedifferentiation within the malignant cell mass. These secondary mutations are relevant for the tumor to gain advantage over neighboring cells and to invade further the local tissue and organs. In the transition from a normal cell to a malignant cell, the modification of intracellular pathways related to cell-cell adhesion and cell-matrix adhesion are important and determine the compactness of the tumor surface and the invasiveness of the tumor (1). Cadherins are cell-cell adhesion proteins which form part of multiprotein complexes at the cell membrane to bind neighboring cells and determine the tissue architecture. The different types of cadherins are named from the type of tissue where they originate from, e.g., E-cadherin in epithelia, N-cadherin in the nervous system, etc. Of particular interest is E-cadherin, sometimes considered as a tumor suppressor protein due to its functionality in maintaining the compactness of the epithelium. The role of E-cadherin in the malfunction of cell-cell adhesion observed in colorectal cancer, and in the β-catenin degradation system after mutations that affect the *wnt*-pathway, belong to the most studied examples (2–4). Greater than 80% of colorectal tumors show malfunctions in APC, a key protein in the *wnt*-pathway related also to intracellular interactions where E-cadherin plays a main role. These mutations are correlated with higher cancer invasion and therefore poorer prognosis.

Mathematical modeling of cell adhesion has been approached by different strategies including continuum models (5,6) (for a general review of mathematical continuum models of cancer see (7)), individual-based lattice-free models (8,10–12) and lattice-based models where each lattice site can at most be occupied by one single cell (13–15) (for general reviews of individual-based models, see (16–19)). Although all these different approaches have shown the importance of cell adhesion to keep tumor compactness and prevent invasion, there is still a wide field to explore linking the intracellular dynamics of signaling pathways to the adhesion molecules at the cell surface and the extracellular consequences in invasive tumors. In this article, we approach this problem using a multiscale individual-based lattice-free model which accounts for the intracellular dynamics of the E-cadherin-β-catenin interactions and the physical forces on the cells.

THE BIOLOGICAL BACKGROUND

When a cell adheres to adjacent neighbors, the E-cadherin molecules are situated in an intermembrane position, forming bonds with local neighbors at the intercellular space. The cytoplasmatic tail of the E-cadherin molecule binds to the proteins of the catenin family: $p120$-catenin, α-catenin, and β-catenin. The α-catenin and β-catenin then form a complex to link the actin filaments of the cytoskeleton and the E-cadherins. When bonds are released, caused by intracellular signaling or the effect of mechanical stress, the

Submitted June 11, 2007, and accepted for publication January 3, 2008.

Address reprint requests to Dirk Drasdo, Tel.: 1-39-63-5036; E-mail: dirk.drasdo@inria.fr; and Ignacio Ramis-Conde, ignacio.ramis_conde@inria.fr.

Editor: Byron Goldstein.

0006-3495/08/07/155/11 $2.00

doi: 10.1529/biophysj.107.114678

multiprotein complex is broken and the E-cadherins are internalized, i.e., transported into the cytoplasm by the endocytosis apparatus within cadherin-coated vesicles. It is not well known yet if, after being endocytosed, E-cadherins are degraded or if they are kept by the vesicles for later recycling (20).

When the bond is broken, β-catenin is released in a phosphorylated state. In this form, it is ready to interact with other molecules and can be recognized and degraded in the proteasome systems. Intracellular control of β-catenin concentration is important in preserving the tissue architecture. Upregulation of free β-catenin (also known as soluble β-catenin) is related to cell migration and the epithelial-mesenchymal transition (22,23), a process where a well-ordered and polarized layer of cells changes into an unstructured configuration to facilitate collective cell migration. Sufficiently large concentrations of soluble β-catenin then move from the cytoplasm into the nucleus, where it interacts with transcription factors which modify cell behavior—for example, by promoting cell proliferation. Although the precise mechanisms which relate the β-catenin nuclear translocation to cell migration are not yet very well known, it has been observed that invasive cells show a higher nuclear accumulation of soluble β-catenin. Wong and Gumbiner (22) used matrigel chambers and different cell chimeras to show how upregulation of soluble β-catenin induces cell migration. They used cell clones with different malfunctions in the cytoplasmatic tail of E-cadherin and found that invasion was enhanced when β-catenin was not able to bind E-cadherin, despite cell-cell bonds being formed at the extracellular part where it was intact. Different biological mechanisms capable to trigger invasion after activating the β-catenin pathway have been proposed (24–26). In particular, Kemler et al. (27) proposed that β-catenin is translocated into the nucleus above a certain concentration threshold leading to downregulation of E-cadherin-mediated adhesion, partly referring on earlier work by Huber et al. (25) and Jamora et al. (28).

In this article, we study the possible effects of a nuclear upregulation of soluble β-catenin as a consequence of being released from the E-cadherin-β-catenin complex, and the biological consequences of the existence of a β-catenin threshold which may downregulate cell adhesion during the epithelial-mesenchymal transition. Instead of considering the pathways that involve β-catenin in every detail known, we focus on a simplified β-catenin pathway which captures the key features of the cell adhesion process. The main interactions of β-catenin in our model are with the E-cadherins at the cell membrane and a generic proteasome-related complex in the cytoplasm which accounts for the whole set of proteins involved in the process of β-catenin degradation. We include soluble β-catenin and the E-cadherin-β-catenin complex as the main variables of our model. Upregulation of soluble β-catenin is assumed to interact with transcription factors in the nucleus, and induce cell migration (26).

THE β-CATENIN KINETICS

We first present our model of the intracellular β-catenin dynamics and show the importance of this regulation system on the E-cadherin system. This is then followed by our single-cell model and a subsection on how the intracellular dynamics couples to the cell-biophysical and cell-biological single-cell parameters.

It is not completely known how E-cadherin is transported from the cytosol to the intermembrane position to form bonds (29). However, there is some evidence that cytoplasmatic E-cadherin translocates to the membrane after binding to β-catenin at the endoplasmic reticulum (30). For simplicity, we assume that the complexes are formed in the cell membrane. This is translated into our model considering three possible different states of the E-cadherins: catenin free in the cytoplasm ($[E_c]$), catenin free at the cell membrane ($[E_m]$), and the complex E-cadherin-β-catenin forming bonds at the cell membrane ($[E/\beta]$). As one cell comes into contact with another cell, the cadherin in the cytoplasm moves to the cell surface. Here we make the assumption that the amount of cadherin stimulated to move is proportional to the contact area. At the cell membrane, the cadherin binds to β-catenin and the cell forms bonds with its neighboring cells. On the other hand, if cell detachment occurs, then the β-catenin-E-cadherin complex is ruptured, the β-catenin becomes soluble β-catenin, and E-cadherin is sequestered into the cytoplasm by endocytosis. Further, we assume that E-cadherin can be recruited to form bonds again. In this way we can consider the total E-cadherin concentration ($E_T = 100$ nM) to be constant:

$$E_T = [E_c] + [E_m] + [E/\beta]. \tag{1}$$

The other reactions described above can be written as

$$[E_c] \rightarrow_{\{\text{contact}\}} [E_m], \tag{2}$$

$$[\beta] + [E_m] \xrightarrow{\nu} [E/\beta], \tag{3}$$

$$[E/\beta] \rightarrow_{\{\text{detachment}\}} [E_c] + [\beta]. \tag{4}$$

Fig. 1 summarizes the intracellular interactions of the different forms of E-cadherin. (We also considered the backward reaction in Eq. 3 and found that it neither modifies the β-catenin steady-state concentrations within a cell, nor changes the multiscale qualitative dynamics as we validated by fixed point analysis and by computer simulations). Following Lee et al. (31), we assume that the production of β-catenin occurs at a constant rate ($k_m = 0.01$ nM min^{-1}). The degradation process takes place after forming a complex with the proteasome. In the framework of our model, this proteasome variable should be understood as a complex of proteins which, after different biochemical interactions, degrade soluble β-catenin, i.e.,

$$[\beta] + [P] \underset{k^-}{\overset{k^+}{\rightleftharpoons}} [C] \xrightarrow{k_2} [P] + \omega, \tag{5}$$

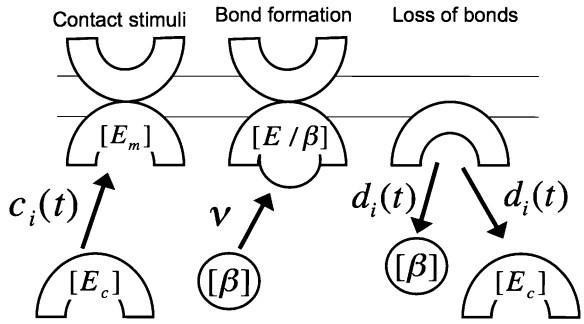

FIGURE 1 The three states of E-cadherin considered in the model: free in the cytoplasm, just arrived to the cell membrane and forming bonds in a multiprotein complex which includes β-catenin. When two cells become in contact, the cadherin travels to the membrane determined by the function $c_i(t)$, it binds, between other molecules, to β-catenin and forms a bond with the neighbor cell. When detachment occurs, the complex β-catenin-E-cadherin is broken at a rate governed by the function $d_i(t)$.

where $[P]$ denotes the concentration of proteasome, $[C]$ is the concentration of β-catenin-proteasome complex, and ω is the final product of the degradation process. The important *wnt*-pathway is taken into account within this degradation process in a very simple way: if *wnt* is activated, and therefore β-catenin cannot bind to actin and be marked for degradation, degradation is at low levels which, in our model, are equivalent to $k^+ \approx 0$. If *wnt* is not activated, β-catenin can be degraded and therefore downregulated.

In a similar way to the E-cadherin concentration, we assume that the proteasome total concentration remains constant ($P_T = 0.33514$ nM), and therefore

$$P_T = [C] + [P]. \tag{6}$$

Using mass conservation we obtain the following system of reaction equations from the above chemical reactions for each individual cell i,

$$d_t[E_c] = -c_i(t)[E_c] + d_i(t)[E/\beta], \tag{7}$$

$$d_t[E/\beta] = \nu(E_T - [E_c] - [E/\beta])[\beta] - d_i(t)[E/\beta], \tag{8}$$

$$d_t[\beta] = -\nu(E_T - [E_c] - [E/\beta])[\beta] + d_i(t)[E/\beta] - k^+ \times [\beta](P_T - [C]) + k^-[C] + k_m, \tag{9}$$

$$d_t[C] = k^+[\beta](P_T - [C]) - k^-[C] - k_2[C], \tag{10}$$

where $\nu = 100\ \text{min}^{-1}$ is the rate at which the complex $[E/\beta]$ is produced, and $k^+ = 100\ \text{min}^{-1}$ and $k^- = 19\ \text{min}^{-1}$ are the β-catenin-proteasome association and dissociation rates, respectively. The functions $c_i(t)$ and $d_i(t)$ measure the amount of cadherin stimulated to form bonds by physical contact with neighboring cells. The function $c_i(t)$ is defined as

$$c_i(t) = \sum_{\text{new contacts}} a_{c,j}(t)\rho_c,$$

where $a_{c,j}(t)$ models the change of area of newly formed cell-cell contacts of cell i with its local neighbors j. $\rho_c = 200$ determines how fast E-cadherin translocates from the cytoplasm to the intermembrane position when induced by cell-cell contact stimuli. The function $d_i(t)$ describes the equivalent effect if detachment occurs, i.e.,

$$d_i(t) = \sum_{\text{new detachments}} a_{d,j}(t)\rho_d,$$

where $a_{d,j}(t)$ models the change of area by lost cell-cell contacts of cell i with its local neighbors j. $\rho_c = 200$ determines how fast E-cadherin translocates from the intermembrane position to the cytosol after cell-cell detachment.

The functions $a(t)_{c,j}$ and $a(t)_{d,j}$ determine the area stimulated to interchange the cadherin from the cytosol to the membrane and from the membrane to the cytosol, respectively. We define these functions as

$$a_{c,j}(t) = \begin{cases} \dfrac{\partial}{\partial t}\hat{a}(t)_j, & \text{if } \dfrac{\partial}{\partial t}\hat{a}(t)_j > 0, \\ 0, & \text{otherwise,} \end{cases}$$

and

$$a_{d,j}(t) = \begin{cases} \left\| \dfrac{\partial}{\partial t}\hat{a}(t)_j \right\|, & \text{if } \dfrac{\partial}{\partial t}\hat{a}(t)_j < 0, \\ 0, & \text{otherwise,} \end{cases}$$

where $\hat{a}(t)_j$ is the approximated contact area between cells i,j at time t divided by the surface area of cell i, calculated by the spherical caps in contact (this approximation has also been used in Galle et al. (8)).

Hence, both attachment and detachment of cells lead to an exchange of E-cadherin between the membranes in the contact zone of the interacting cells. We assume that Eqs. 8 and 9 determine the concentrations of β-catenin and β-catenin-E-cadherin only as long as the soluble β-catenin concentration is below a threshold c_T. In the case $[\beta] > c_T$, we consider the soluble β-catenin in cytoplasm to be large enough and as a consequence it is free to enter the nucleus and interact with transcription factors causing the cell to migrate. As a necessary step of migration, cell detachment occurs. To model the active detachment process we assume that for $[\beta] > c_T$,

$$d_t[E/\beta] = -(\alpha + d_i(t))[E/\beta], \tag{11}$$

$$d_t[\beta] = (\alpha + d_i(t))[E/\beta] - k^+[\beta](P_T - [C]) + k^-[C] + k_m, \tag{12}$$

replace the original Eqs. 8 and 9, respectively. The value α is the rate at which the complex is dissociated once the migration decision has been made.

Since the molecular kinetics of β-catenin and its interaction varies between different cells, each cell within our model is considered as an individual entity which intracellular dynamics are governed by the explained equations. Motivated by the observations that cells in isolation tend to aggregate (32), we assume that an invasive cell changes into a noninvasive state again if it comes into contact with other cells to which it can attach. In this case, Eqs. 8 and 9 are recovered.

The intracellular parameters values were taken, when possible, from Lee et al. (31). Any others were chosen in a similar range to the ones they used. All the parameters values are given in Table 1.

TABLE 1 Parameter values used in the intracellular simulations

Parameter	Definition	Value	Source
ν	E-cadherin-β-catenin binding rate	100 min^{-1}	Estimated*
k^+	β-catenin proteasome normal binding rate	100 min^{-1}	Estimated*
k^+	β-catenin proteasome downregulated binding rate	0 min^{-1}	Estimated
k^-	β-catenin-proteasome dissociation rate	19 min^{-1}	Estimated*
k_2	β-catenin degradation rate in proteasome	0.03 min^{-1}	Estimated*
k_m	β-catenin production rate	0.01 nM/min^{-1}	(31)
P_t	Proteasome total concentration	0.33514 nM	Estimated*
E_t	E-cadherin total concentration	100 nM	Estimated*
ρ_i	E-cadherin surface translocation rate	200 min^{-1}	Estimated*
α	E-cadherin-β catenin dissociation rate	2 min^{-1}	Estimated
c_T	β-catenin threshold value	$c_T = 50$	Estimated
R_0	Cell radius	5 μm	(8)
E	Young modulus	1 kPa	(8)
ν	Poisson ratio	1/3	(8)
$\gamma_{\parallel}$	Parallel friction constant	0.5*10^{11} Ns/m^3	(8)
$\gamma_{\perp}$	Perpendicular friction constant	0.5*10^{11} Ns/m^3	(8)
W_s	Adhesion energy	200 μN/m	(8)
γ	Cell-medium friction constant	0.4 Ns/m^3	(8)
D	Cell diffusion constant	10^{-12} cm^2/s	(8)

When possible, the parameters were taken from literature.
*Those intracellular parameters not found in experimental data were assumed to maintain the β-catenin steady value at 35 nM as observed by Lee et al. (31).

THE BIOPHYSICAL MODEL OF A SINGLE CELL

We model each cell as an isotropic elastic object capable of migration and division and parameterize it by cell-kinetic, biophysical and cell-biological parameters that can be experimentally measured. We now describe below the key features of this modeling approach.

Cell-cell shape

We assume that an individual cell in isolation is spherical. We characterize the cell shape of a spherical cell by its radius R.

Cell division

In our model the cell cycle is subdivided into two phases—the interphase and the mitotic phase. We assume that during interphase the cell doubles its mass. In the mitotic phase a cell divides into two daughter cells. We model the process of cell division by replacing two cells of size R by two daughter cells of radius $R/2^{1/3}$ which then gradually grow during interphase to their original radius R. This radius value to determine the size of the new daughter cells was taken in according to the simulations performed by Galle et al. (8), where they reproduced realistic tumor growth curves using an individual force-based model of similar characteristics to ours.

Cell-cell interaction

With decreasing distance between the centers of two cells (e.g., upon compression), both their contact area and the number of adhesive contacts increase, resulting in an attractive interaction. On the other hand, if cells are spheroidal in isolation, a large contact area between them significantly stresses their cytoskeleton and membranes. Furthermore, experiments suggest that cells only have a small compressibility (the Poisson numbers are close to 0.5 (33,34)). In this instance, both the limited deformability and the limited compressibility give rise to a repulsive interaction. We model the combination of the repulsive and attractive energy contributions by a modified Hertz-model (8,10) where the potential V_{ij} between two cells of radius R_i and R_j is given by

$$V_{ij} = \underbrace{(R_i + R_j - d_{ij})^{5/2}\frac{1}{5\tilde{E}_{ij}}\sqrt{\frac{R_i R_j}{R_i + R_j}}}_{\text{repulsive contribution}} + \underbrace{\epsilon_s}_{\text{adhesive contribution}}. \quad (13)$$

The first term of the equation models the repulsive interaction, the second term the adhesive interaction, and $\tilde{E}_{ij}$ is defined by

$$\tilde{E}_{ij}^{-1} = \frac{3}{4}\left(\frac{1-\sigma_i^2}{E_i} + \frac{1-\sigma_j^2}{E_j}\right). \quad (14)$$

Here, E_i, E_j are the elastic moduli of the cells i, j, σ_i, σ_j the Poisson ratios of the spheres. $\epsilon_s \approx \varrho_m A_{ij} W_s$, where $W_s \approx 25\, k_B T$ (T, temperature; k_B, Boltzmann constant) is the energy of a single bond, A_{ij} the contact area between cells i, j, and ϱ_m is the density of surface adhesion molecules in the contact zone, in our case the density of $[E/\beta]$ (35). The interaction force results from deriving the potential function

$$\underline{F}_{ij} = -(\partial V_{ij}/\partial d_{ij})(d(d_{ij})/dx,\, d(d_{ij})/dy,\, d(d_{ij})/dz). \quad (15)$$

The modified Hertz-model approximates a cell as an elastic sphere and superimposes the repulsive force that emerge in case of a deformation or compression of the sphere with an

attractive contribution due to cell-cell adhesion. In some cancer cell lines a hysteresis effect has been observed, i.e., the attachment and detachment of cells occur at different distances between the cell centers (21). However, Drasdo et al. (9) have shown that the effect of the hysteresis is only a delay in the detachment, while the qualitative behavior of the detachment process does not depend on the existence of the hysteresis. The advantage of the modified Hertz model is that both the interaction energy and the force can be represented as an analytical expression, while for models that represent the hysteresis effect such as the Johnson-Kendall-Roberts model, the force has to be calculated numerically from an implicit equation.

Cell movement

We model cell movement by a stochastic equation of motion for each cell. Alternatively, the Metropolis-algorithm has been used in Drasdo and Hoehme (11). The direct use of equations of motion for the cells permits one to include more easily the limiting case of very small (or no) noise and is more intuitive. In this approach, cells move under the influence of forces and a random contribution to the locomotion which results from the local exploration of space. Moreover, in some of the scenarios explained below, a chemoattractant chemical generates a forcelike term in the Langevin equation as suggested in Stevens (36):

$$\underbrace{\underline{\underline{\Gamma}}^{\mathrm{f}}_{\mathrm{is}}\underline{v}_{\mathrm{i}}}_{\text{s-friction}} + \underbrace{\sum_{\mathrm{j\,nn\,i}}\underline{\underline{\Gamma}}^{\mathrm{f}}_{\mathrm{ij}}(\underline{v}_{\mathrm{i}}-\underline{v}_{\mathrm{j}})}_{\text{cell-cell friction}} = \underbrace{\sum_{\mathrm{i\,nn\,j}}\underline{F}_{\mathrm{ij}}}_{\text{forces}} + \underbrace{\underline{f}_{\mathrm{i}}(t)}_{\text{noise}} + \underbrace{\chi\underline{\nabla}Q(t)}_{\text{chemotaxis}}. \tag{16}$$

Inertia terms have been neglected due to the high friction of cells with their environment, and we also do not consider the existence of any memory term, as in Galle et al. (8). The value $\underline{v}_{\mathrm{i}}$ is the velocity of the cell i at time t, $\underline{F}_{\mathrm{ij}}$ is the force of cell j on cell i (previously calculated from Eqs. 13 and 14) and the sums are over the nearest neighbors in contact with cell i. The s-friction term determines the friction with the substrate and the cell-cell friction determines the friction with the nearest neighbors. The tensors $\underline{\underline{\Gamma}}^{\mathrm{f}}_{\mathrm{ij}}$ and $\underline{\underline{\Gamma}}^{\mathrm{f}}_{\mathrm{is}}$ denote cell-cell friction and cell-substrate friction, respectively. In our model, cells are considered to be spherical and to be surrounded by a homogeneous and isotropic environment, either a gel or a homogeneous intracellular matrix, depending on the experimental situation under consideration. Under these assumptions, the cell-substrate friction tensor takes the form

$$\underline{\underline{\Gamma}}^{\mathrm{f}}_{\mathrm{is}} = \gamma\underline{\underline{I}},$$

where $\underline{\underline{I}}$ denotes the identity matrix and γ is the friction coefficient of the medium. The cell-cell friction is described by the tensor (9)

$$\underline{\underline{\Gamma}}^{\mathrm{f}}_{\mathrm{ij}} = \gamma^{(\mathrm{ij})}_{\parallel}\underline{n}_{\mathrm{ij}}\underline{n}_{\mathrm{ij}} + \gamma^{(\mathrm{ij})}_{\perp}(\underline{\underline{I}} - \underline{n}_{\mathrm{ij}}\underline{n}_{\mathrm{ij}}).$$

The values $\underline{x}_{\mathrm{i}}$ and $\underline{x}_{\mathrm{j}}$ are the position of the center of mass of the cells and $\underline{n}_{\mathrm{ij}} = (\underline{\mathrm{x}}_{\mathrm{j}} - \underline{\mathrm{x}}_{\mathrm{i}})/|\underline{\mathrm{x}}_{\mathrm{j}} - \underline{\mathrm{x}}_{\mathrm{i}}|$. The value $\underline{n}_{\mathrm{ij}}\underline{n}_{\mathrm{ij}}$ here denotes the dyadic product, i.e., it is a 3×3-matrix. The values $\gamma^{(\mathrm{ij})}_{\parallel}$ and $\gamma^{(\mathrm{ij})}_{\perp}$ are the parallel and perpendicular friction constants, respectively. The force term is the force that cell i exerts on the other cells in contact with it. The noise term models the random component in the cell movement (the micromotility) and is chosen to be uncorrelated as explained in the literature (8,9), i.e.,

$$\langle\underline{f}(t)\underline{f}(t')\rangle \approx 2\underline{\underline{\hat{\Gamma}}}\delta(t-t')$$

and zero mean

$$\langle\underline{f}(t)\rangle = 0.$$

The value $\underline{\underline{\hat{\Gamma}}}$ denotes the amplitude of the autocorrelated noise. Here we approximate $\underline{\underline{\hat{\Gamma}}} \approx 2\gamma^2 D\underline{\underline{I}}$. The value D is the diffusion constant and characterizes the free random movement of isolated cells in the medium. Typically, $D \approx 10^{-12}$ cm^2/s.

The chemotaxis term is the chemotactic/haptotactic response toward a gradient of morphogen $Q(t)$ and χ is the cell sensitivity to the chemical. This last term is only included in some of our simulations scenarios as is specified below.

COUPLING OF CELL PARAMETERS TO INTRACELLULAR MOLECULE CONCENTRATIONS

In our model, the adhesion forces between cells are controlled by the density of E-cadherin in the cell membrane within the cell-cell contact zone. We could not find in the literature specific values for E-cadherin concentration per cell-cell bond. In their simulations Galle et al. (8), used an adhesion energy per unit of area of $W_{\mathrm{s}}\varrho_{\mathrm{m}} = 200\,\mu\,\mathrm{Nm}^{-1}$, so that the surface receptor density is $\varrho_{\mathrm{m}} = 200\,\mu\,\mathrm{Nm}^{-1}\,W_{\mathrm{s}}^{-1}$. We use this value as a maximum density of the cadherin-β-catenin complex in the membrane and define the actual density by

$$\varrho = \frac{[E/\beta]}{E_{\mathrm{T}}}\varrho_{\mathrm{m}}.$$

In our simulations we nondimensionalize all cadherin concentrations by E_{T}, so that the nondimensional concentrations of free E-cadherin in the cytoplasm and in the membrane, and of E-cadherin within E-cadherin-β-catenin complexes, are all in the interval [0, 1].

Fig. 2 shows the resulting force function depending on the different $\varrho^{\mathrm{ij}}_{\mathrm{m}}$ values. By modifying the intracellular concentration of β-catenin the cells can control the concentration of $[E/\beta]$-complexes and thereby the strength of the intercellular adhesion force.

The active decision of a cell to migrate can be triggered in different ways, all of them involving an upregulation of the soluble β-catenin which overcomes the critical threshold c_{T}. One case happens if the cytoplasmic concentration of β-catenin is upregulated due to a failure in the proteasome

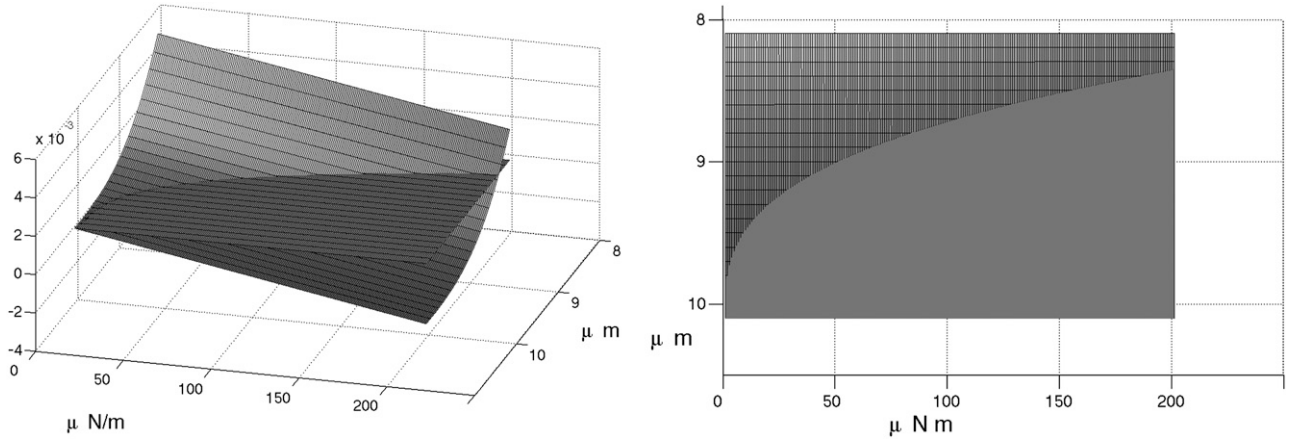

FIGURE 2 The left plot shows the force function between two cells, variables are distance between the centers of the cells (in μm) and adhesion energy per unit of area in contact (in μN/m). The right plot shows the vertical view of the same graph, where it can be better observed the adhesive interaction between cells depending on the E-cadherin concentration forming bonds. The gridded part determines the zone where adhesive forces act.

system. A further case happens if the detachment of local neighbors upregulates the soluble β-catenin concentration. In both cases, β-catenin enters the nucleus and triggers cell migration. One way that this could cause rupture of the cell-cell contacts is by physical forces that a cell that starts to migrate exerts on the cadherin bonds in the cell-cell contact area to its neighbors. In our simulations, we have chosen the last term in Eq. 16 that represents chemotaxis so large that the cells at the tumor surface were not able to detach by breaking the cell-cell contacts but they need to downregulate their adhesion molecules. However, detachment could also be triggered by an increase of the intrinsic random movement component of a cell represented by the noise term which we do not consider here.

RESULTS

In this section, we present the results of computational simulations carried out on our model given by Eqs. 7–12 and 16. In the first set of simulations in Figs. 3 and 4, we present results from a numerical simulation of the system of ordinary differential Eqs. 7–12 governing the concentrations of various forms of E-cadherin, β-catenin, and the proteasome in a single cell.

To illustrate the response of possible malfunctions in the intracellular control on the β-catenin concentration, we study simulations for different attachment/detachment scenarios. If the cell remains adhered to its neighbors, almost all of the β-catenin remains bound to the E-cadherin complexes at the cell membrane. If a cell detaches, then the concentration of soluble β-catenin increases.

Fig. 3 shows the concentration of the intracellular variables of a single cell when it attaches other cells; as can be seen from the figure, soluble β-catenin (*dotted line*) is rapidly sequestered from the cytoplasm by the cadherins to form the $[E/\beta]$ complex (*solid line*). As long as the contacts are maintained, the soluble β-catenin concentration remains at a low level. If some of the neighboring cells detach, then the concentration of E-cadherin forming bonds will be partially reduced.

Fig. 4 shows concentrations of the intracellular variables for two different detachment scenarios. In the figure on the left, we assume that the cell loses all its bonds with the neighbors at $t \approx 0.4$, which triggers a dramatic increase of the β-catenin concentration in the cytoplasm. This soluble β-catenin enters the nucleus in excess of the threshold concentration necessary to initiate migration and promote cell movement via transcription. On the right figure, at time $t \approx 0.4$, the cell has lost only one-quarter of its bonds with the neighbors and the soluble β-catenin concentration is insufficient to cause cell migration.

We implement the intracellular dynamics model explained above in every single cell of the individual-force-based model. The advantage of using this type of modeling

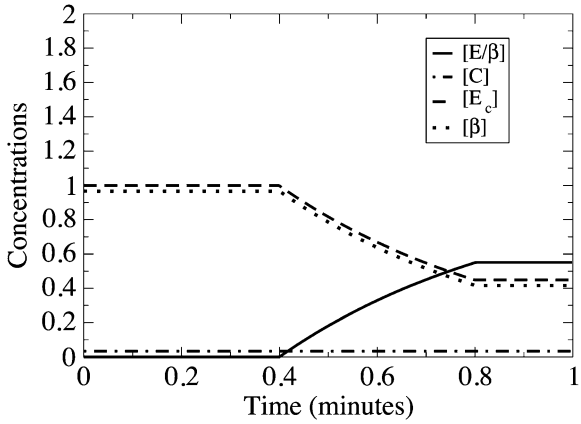

FIGURE 3 Plot showing the concentrations over time of the intracellular variables of a cell that attaches to a group of cells at $t \approx 0.4$ min. The β-catenin is rapidly sequestered by the cadherins that travel to the cell surface to form bonds.

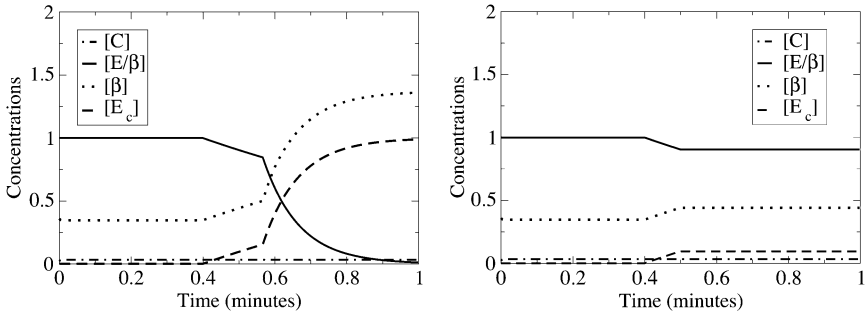

FIGURE 4 Plots showing the concentrations over time of the intracellular variables under two different scenarios. On the left plot, a cell loses its contact with its neighbors at $t \approx 0.4$ min. The β-catenin concentration increases dramatically and it enhances mechanisms which promote invasion. On the right plot only a few of the neighbors are detached, soluble β-catenin is maintained under the threshold levels ($c_T = 0.5$) that enhances migration.

approach is that not only does it enable us to explicitly include the influence of intracellular pathways, but also provides a realistic approach to model the biophysical properties of individual cells which cannot be neglected when studying tissue organization. We reproduce in silico different scenarios of relevance in cancer growth and invasion and study the behavior of detachment waves in epithelial layers and how it can produce the epithelial-mesenchymal transition. We also study the β-catenin distribution in small tumors and how its upregulation can induce invasion.

Detachment waves in epithelial layers

Figs. 5 and 6 show the spatio-temporal dynamics in a hexagonal lattice of the cells soluble β-catenin concentration, similar to the natural configuration of an epithelial layer. We choose here a tissue architecture where we have a layer of cells, with each cell in the layer being attached to each neighboring cell, and initial values of E-cadherin and β-catenin at the steady state for the intracellular model. The intracellular concentration of β-catenin is denoted by the color of the cell: white denotes high concentration of soluble β-catenin and black low. We note that as we have assumed that high concentrations of β-catenin induce cell-cell detachment, this occurence of colors is equivalent to saying that black denotes strong cell adhesion and white denotes weak cell adhesion. Within the cell layer, we insert a cell which has no regulation activity in the β-catenin pathway (we force its intracellular dynamics to rise $[\beta] > c_T$ after a certain time and therefore detach from its nearest neighbors). Fig. 5 shows how this malfunction produces a wave caused by the intracellular upregulation of β-catenin in the nearest neighbors. In the way this wave front is moving, it can be observed how it induces a temporal cell-cell detachment within the whole epithelial layer. A particular feature of these waves that should be highlighted is the fact that they do not satisfy the principle of superposition.

The epithelial mesenchymal transition

Fig. 7 shows how the three-dimensional spatio-temporal dynamics influence cell migration in a scenario where cells migrate away from a two-dimensional epithelial layer to produce the epithelial-mesenchymal transition. The so-called epithelial-mesenchymal transition is a process where a well-polarized layer of cells become diffuse and lose their initial structure and compactness. This transition occurs in a similar

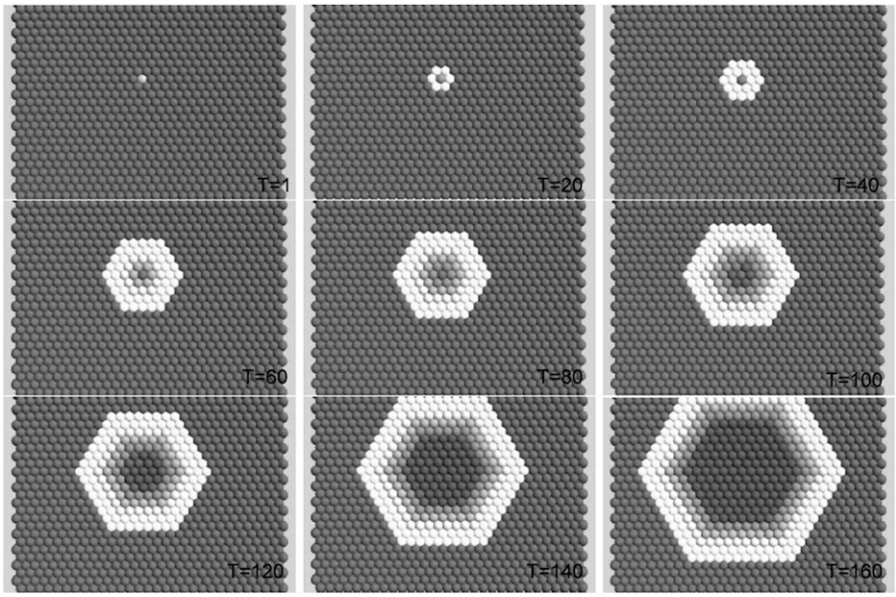

FIGURE 5 Plots of the spatio-temporal dynamics of $[\beta]$ in a layer of cells where a single cell with upregulated soluble catenin (*white*) is situated on a layer with defective proteasome system. As can be seen from the plots, it produces a wave of upregulated β-catenin (*white*) caused by the induced decision of detachment in other cells. After the wave has passed, strong adhesion is recovered (*black*). Unit of time is measure in minutes.

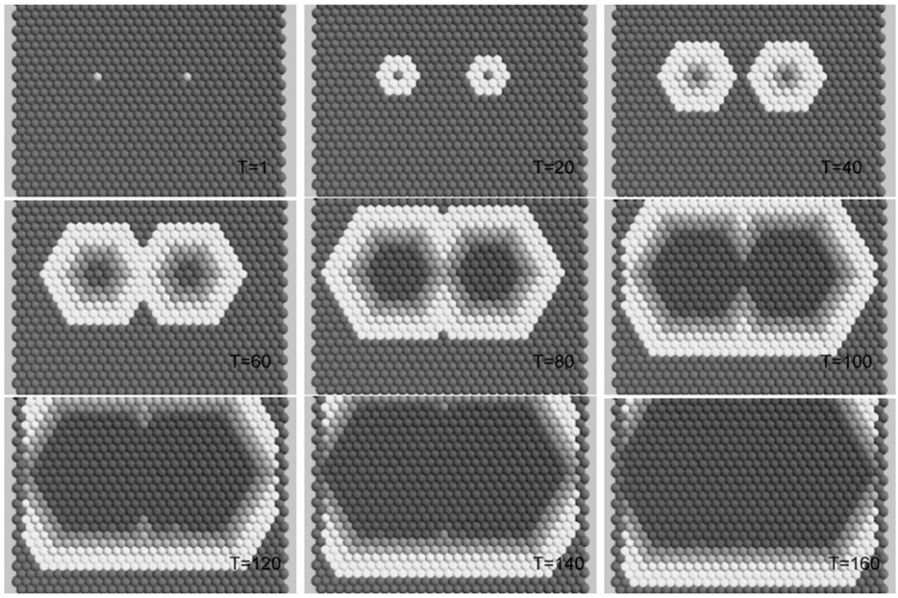

FIGURE 6 Plots showing the spatio-temporal dynamics of a scenario where two cells with up-regulated soluble β-catenin are situated on a layer with defective proteasome system (*white*), inducing two detachment waves. The detachment waves collide and vanish. This outcome prevents the cell layer to become disorganized due to an excess of detachment signal. Unit of time is measured in minutes.

way at the tumor surface when invasion occurs—the mass of outer cells lose contact and invade further into the tissue. To model the epithelial-mesenchymal transition, we set as initial conditions a layer of cells where the outermost cells are fixed (i.e., unable to move). We include a constant force term as if it were a constant source of chemoattractant (term 5 in Eq. 9) that diffuses toward the tissue in the form of the equation

$$\frac{\partial Q(t)}{\partial t} = D_{\mathrm{Q}} \Delta Q(t).$$

Fig. 7 shows how the cells migrate and the configuration of the epithelial layer is lost. When the proteasome system is downregulated and a cell detaches it induces the same behavior in neighboring cells, creating a mass of migrating cells. This is a very similar outcome to the epithelial-mesenchymal transition. The same migration mechanism can be observed in a small tumor—cells detach from the outer rim and migrate toward a source of attractants (see Fig. 10).

Tumor growth, aggregation and invasion

Figs. 8 and 9 show the distribution of soluble catenin in a two-dimensional cross section of a three-dimensional tumor, and a two-dimensional aggregation process of a culture of metastatic cells on a petri dish. The process of tumor growth involves different cellular interactions which alter and remodel the E-cadherin configuration at the cell surface with a subsequent impact on β-catenin concentration. In a proliferative

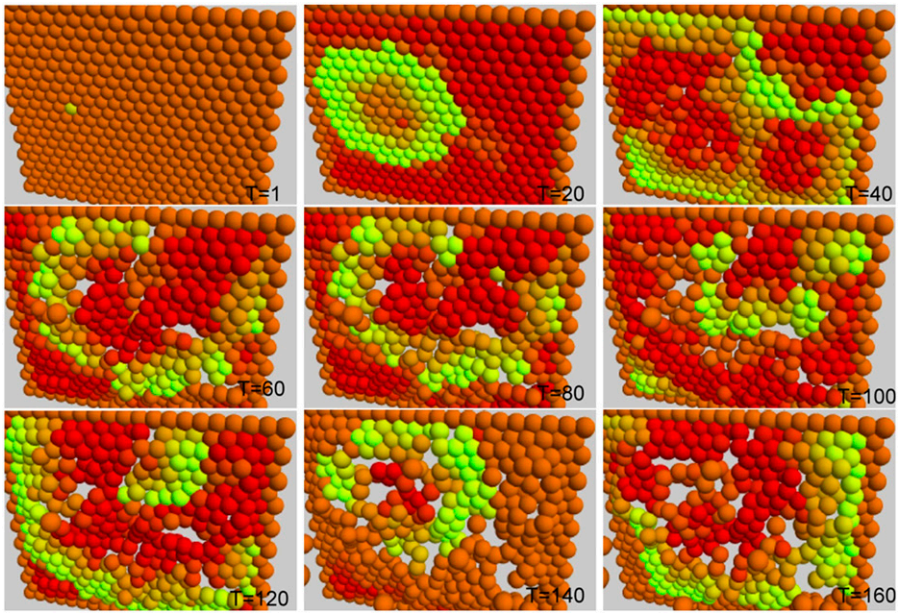

FIGURE 7 Plots showing how malfunctions in the proteasome system can alter the layer configuration producing the epithelial-mesenchymal transition. In this figure, the cells migrate toward a source of attractants escaping from the initial epithelial configuration. Migration can occur only when the catenin levels are over a determined threshold (*yellow*). Unit of time is measured in minutes.

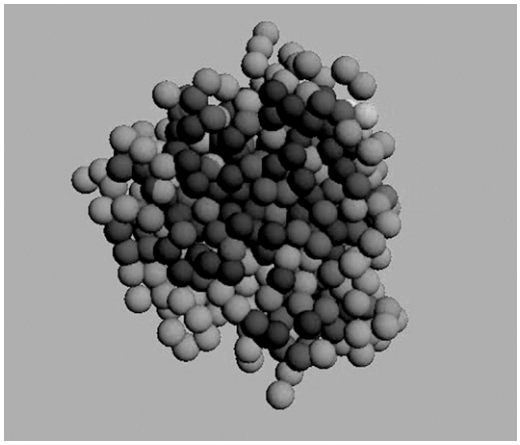

FIGURE 8 Plot showing a transversal section of a tumor shows how the catenin spatial distribution depends on the tumor geometry. Cells in gray have fewer binding neighbors and the catenin concentration is not attached to the cadherins and free to go into the nucleus. Cells in the center of the tumor show how catenin is better downregulated by a larger number of binding neighbors (*black*).

mass of cancer cells, cell detachment, via internal signaling or physical forces, is a necessary process to release the stress and allow the proliferation.

Fig. 8 shows a section of the tumor (*radius* $\approx 100\ \mu$m) where we can observe the different distribution of the intracellular catenin. The outer rim of the growing tumor has a higher number of cells with nuclear β-catenin concentration, while, in the center of the tumor, cells downregulate the intracellular β-catenin concentration when it is sequestered by the E-cadherins forming bonds at the cell membrane. These simulations are in very good agreement with the findings of Brabletz et al. (4).

Fig. 9 shows the same patterns found when we study the aggregation process in two-dimensional layers. These findings show how our model can reproduce not only the epithelial-mesenchymal transition but also recover the compactness of the subsequent distant metastatic clusters via aggregation and growth. If the threshold value c_T is small enough, the same traveling wave patterns as those found in the previous scenarios can be observed within the tumor. For threshold values high enough ($c_T > E_T$), the waves can be avoided but the β-catenin distribution observed by Brabletz et al. (4) remains.

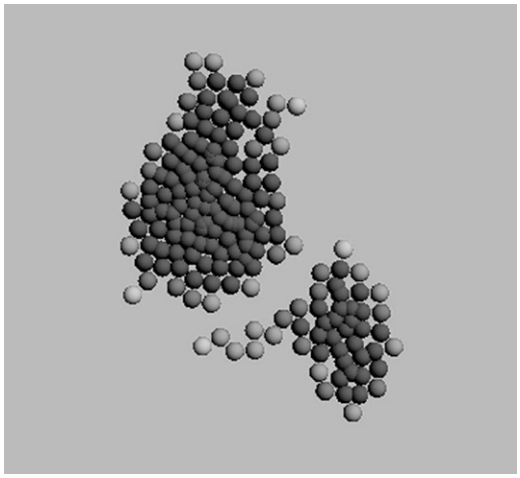

FIGURE 9 Plot showing a scenario where cells aggregate and grow in a two-dimensional configuration in a petri dish where they show similar patterns of β-catenin distribution as those found by Brabletz et al. (4). Clearer cells denote a higher β-catenin nuclear concentration.

In Fig. 10, we show results from the same growing tumor scenario stimulated by a source of chemoattractant. If cell detachment occurs, then cells will migrate toward the source of attractants. The proteasome functionality has been downregulated to the point where migration occurs. It can be observed that the outer cells migrate and detach from the main tumor mass; the new cells at the outer rim lose part of their E-cadherin bonds, upregulate soluble β-catenin, and enhance their migration and invasion. These findings suggest how invasion can be a gradual process produced by subsequent layers of cells that detach the tumor surface.

We performed a steady-state and a sensitivity analysis of the intracellular reaction equations. Table 2 reports the result of the sensitivity analysis. Shown is the percentage of the soluble β-catenin in relation to the steady state obtained for the parameters of Table 1 (e.g., ''100'' means the corresponding value has not changed). The intracellular dynamics is very robust with regard to changes of most parameters. The largest sensitivity has been found for variations of the β-catenin production rate (k_m) and in the proteasome degradation rate (k_2).

The steady states of the β-catenin-proteasome complex and soluble β-catenin are

$$[C_o] = \frac{k_m}{k_2} \tag{17}$$

and

$$[\beta_o] = \frac{[C_o](k^- + k_2)}{k^+(P_t - [C_o])} = \frac{k_m/k_2(k^- + k_2)}{k^+(P_t - k_m/k_2)}, \tag{18}$$

respectively. From Eq. 18, $P_t > [C_o]$, which is satisfied for the chosen parameters values. In agreement with the results obtained from the sensitivity analysis (Table 2), the soluble β-catenin concentration at the steady state is controlled by the degradation rate of the β-catenin-proteasome complex, k_2, if k_2 is large.

We studied the dependency of the multiscale dynamics on the intracellular β-catenin degradation rate (k_2). We simulated an invasion assay of similar characteristics to the ones performed by experimentalists in matrigel chambers (22). The initial conditions were taken as in the scenario simulated in Fig. 10 where a growing tumor is stimulated by a source of chemoattractant. We performed the migration assay for three different degradation rates: fast ($k_2 = 10\ \text{min}^{-1}$), medium ($k_2 = 1\ \text{min}^{-1}$), and no degradation ($k_2 = 0\ \text{min}^{-1}$), and plot over time the number of cells achieving escape from the

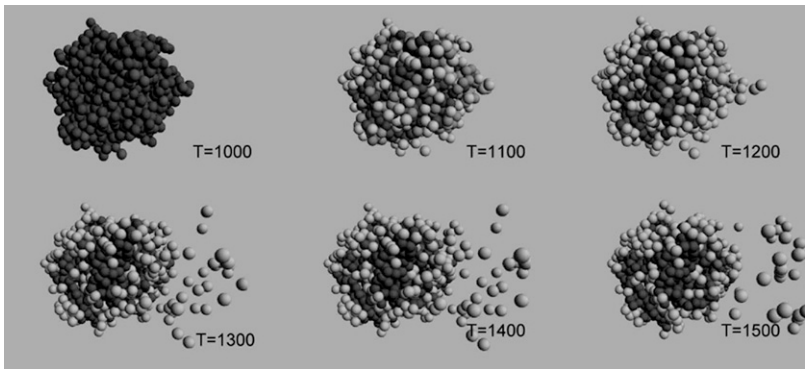

FIGURE 10 Plot showing how a small tumor invades further tissue stimulated by a source of morphogen located at the right-hand side of the tumor. Cells decide to detach gradually when the intracellular concentration of β-catenin is upregulated (*light gray*). Unit of time is measure in minutes.

initial tumor to a distance of 150 μm. Fig. 11 shows the results of the migration assay. It can be seen that the intensity of degradation activity of the proteasome determines the capacity of invasion of the malignant cells.

DISCUSSION

In this section, we have studied the intracellular and extracellular dynamics that would cause a possible soluble β-catenin upregulation via the release of E-cadherin bonds. As a framework, we used a similar approach to the experiments performed by Brabletz et al. (4), and we have shown the same patterns of intracellular catenin distribution under a growth process and an aggregation process. Brabletz et al. (4), looking at the intracellular concentration of β-catenin, postulated how tumor progression was driven by interactions with the tumor environment. In our findings, we have shown how this interaction may be mainly driven by the tumor cells themselves. We have shown how downregulation of β-catenin can be mainly driven by cell-cell contacts and how this fact gives an invasive advantage to the cells that are positioned at the outer rim of the tumor. We have simulated the different main steps involved in an invasion process and shown how the epithelial-mesenchymal transition can be achieved (migration) and reversed (aggregation and growth) depending on the regulation of soluble β-catenin by local contacts.

TABLE 2 Results of the sensitivity analysis performed to study the variation of soluble β-catenin

Parameter	$\times$ 10	$\times$ 10^2	$\times$ 10^{-1}	$\times$ 10^{-2}
ν	100	100	100	100
k^+	99.974	100	101.847	100.200
k^-	100.237	101.234	99.974	99.972
k_2	55.056	0.005	104.502	104.952
k_m	144.900	594.976	95.50	95.054
ρ_i	100	100	100	100
α	100	100	100	100

The values obtained from running simulations in different orders of magnitude are given in percentages with respect to the β-catenin steady-state concentration obtained from substituting the parameters of Table 1 in Eq. 18. (Table 1 denotes the case ''Parameter $\times$ 1'' where each rate is 100%) It can be observed that the intracellular dynamics are very robust with respect to most of the parameters.

More intriguing is how these simple dynamics can create waves of temporal cell-cell detachments. When considering the structure of a human tissue, we have to bear in mind how it is exposed to continuous mechanical stress and remodeling. Cell migration, apoptosis, and cell mitosis are, probably, the three most important events that can alter the physical configuration of the layer. Shimamuram and Takeichi (29) have shown how E-cadherin expression was transient in mouse embryonic brain morphogenesis. They stained different zones of the brain and neural tube and showed how E-cadherin expression followed particular patterns of expression where positive E-cadherin cells were isolated in different configurations from negative E-cadherin cells. To maintain the natural tissue configuration and the stress levels under a threshold that permits cell survival, a local mechanism of signaling and migration of neighboring cells is necessary. This mechanism must allow cells, in attaching and detaching, to find an optimal position such as is seen in an epithelial configuration, but must also be efficient enough to avoid unnecessary detachments and disorganization of the tissue. We do not claim that our model of the internal cell dynamics is the exact model of what actually occurs, but we do wish to highlight how a simple mechanism can show transient

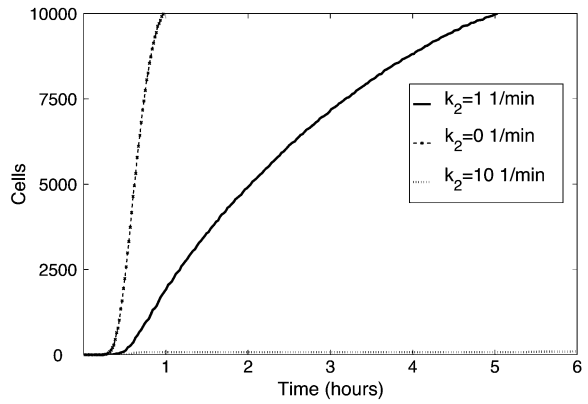

FIGURE 11 Plot showing the simulation results of a cell invasion assay. The plot shows the number of cells that achieve a migration distance of 150 μm away from the principal tumor over time. It can be observed that as the β-catenin degradation rate is decreased (k_2 = 10, 1, and 0 min^{-1}), the malignant cells become more invasive.

catenin/cadherin expression (recall that, in our model, cadherin is surface-expressed when forming bonds) and differentiate the tissue into two separate parts (cadherin/catenin positive and cadherin/catenin negative). In our simulations, we have shown how a mechanism biregulated by cell-cell junctions and an independent degradation system can be sufficient to do this work. When a cell needs to migrate and releases the bonds with its neighbors, a ''traveling wave'' of detachment happens. This wave facilitates the cell layer to reaccommodate and release the stress caused by the new movement. Furthermore, this model produces a self-regulation mechanism—when two waves collide, both of them vanish. This helps to prevent tissue disorganization caused by an excess of signaling. If many cells in the layer are sending detachment signals at the same time, the whole layer will become detached and chaotic; however, if the detachment waves vanish when they collide, each single cell, at one time, releases its bonds as if there were only a single wave.

D.D. acknowledges support by BMBF Hepatosys. No 0313081F.

REFERENCES

1. Chaplain, M. A. J., L. Graziano, and L. Preziosi. 2006. Mathematical modeling of the loss of tissue compression responsiveness and its role in solid tumor development. *Math. Med. Biol.* 23:197–229.
2. Thomas Brabletz, Andreas Jung, Simone Reu, Marc Porzner, Falk Hlubek, Leoni A. Kunz-Schughart, Ruth Knuechel, and Thomas Kirchner. 2001. Variable β-catenin expression in colorectal cancers indicates tumor progression driven by the tumor environment. *PNAS.* 98:10356–10361.
3. Natke, I. S. 2004. The adenomatous, *Polyopsis coli* protein: the Achilles heel of the gut epithelium. *Annu. Rev. Cell Dev. Biol.* 20:337–366.
4. Hardy, R. G., S. J. Meltzer, and J. A. Jankowsky. 2000. ABC of colorectal cancer, molecular basis of risk factors. *Clin. Rev.* 321:886–889.
5. Byrne, H. M., and M. A. J. Chaplain. 1996. Modeling the role of cell-cell adhesion in the growth and development of carcinomas. *Math. Comput. Model.* 24:1–17.
6. Armstrong, N. J., K. J. Painter, and J. A. Sherratt. 2006. A continuum approach to modeling cell-cell adhesion. *J. Theor. Biol.* 243:98–113.
7. Araujo, R. P., and D. L. McElwain. 2004. A history of the study of solid tumor growth: the contribution of mathematical models. *Bull. Math. Biol.* 66:1039–1091.
8. Galle, J., M. Loeffer, and D. Drasdo. 2005. Modeling the effect of deregulated proliferation and apoptosis on the growth dynamics of epithelial cell populations in vitro. *Biophys. J.* 88:62–75.
9. Drasdo, D., S. Hoehme, and M. Block. 2007. On the role of physics in the growth and pattern formation of multi-cellular systems: What can we learn from individual-cell based models? *J. Stat. Phys.* 128:287–345.
10. Schaller, G., and M. Meyer-Hermann. 2005. Multicellular tumor spheroid in an off-lattice Voronoi-Delaunay cell model. *Phys. Rev. E.* 71:051910-1–051910-16.
11. Drasdo, D., and S. Hoehme. 2005. A single-cell based model to tumor growth in vitro: monolayers and spheroids. *Phys. Biol.* 2:133–147.
12. Ramis-Conde, I., M. A. J. Chaplain, and A. R. A. Anderson. 2006. Mathematical modeling of cancer cell invasion of tissue. *Math. Comput. Model.* In press.
13. Anderson, A. R. A. 2005. A hybrid mathematical model of solid tumor invasion: the importance of cell adhesion. *Math. Med. Biol.* 22:163–186.
14. Drasdo, D. 2005. Coarse graining in simulated cell populations. *Adv. Complex Syst.* 2,3:319–363.
15. Block, M., E. Schoell, and D. Drasdo. 2007. Classifying the growth kinetics and surface dynamics in growing cell populations. *Phys. Rev. Lett.* 99:248101–248104.
16. Moreira, J., and A. Deutsch. 2002. Cellular automata models of tumor development—a critical review. *Adv. Complex Syst.* 5:247–267.
17. Alber, M. S., M. A. Kiskowski, J. A. Glazier, and Y. Jiang. 2002. On cellular automaton approaches to modeling biological cells. *In* Mathematical Systems Theory in Biology, Communication, and Finance. J. Rosenthal and D. S. Gilliam, editors. Springer, New York.
18. Drasdo, D. 2003. On selected individual-based approaches to the dynamics of multicellular systems. *In* Multiscale Modeling. W. Alt, M. Griebel, and J. Lenz, editors. Birkhäuser, Basel, Switzerland.
19. Anderson, A. R. A., M. A. J. Chaplain, and K. A. Rejniak (editors). 2007. Single-Cell-Based Models in Biology and Medicine. Birkhäuser, Basel, Switzerland.
20. Pece, S. J., and S. Gutkind. 2002. E-cadherin and Hakai: signaling, remodeling or destruction? *Nat. Cell Biol.* 4:e72–e74.
21. Chu, Y.-S., S. Dufour, J. P. Thiery, E. Perez, and F. Pincet. 2005. Johnson-Kendall-Roberts theory applied to living cells. *Phys. Rev. Lett.* 280:312–315.
22. Wong, A. S. T., and B. M. Gumbiner. 2003. Adhesion independent mechanism for suppression of tumor cell invasion by E-cadherin. *J. Cell Biol.* 161:1191–1203.
23. Friedl, P. 2004. Prespecification and plasticity: shifting mechanisms of cell migration. *Curr. Opin. Cell Biol.* 16:14–23.
24. Nelson, W. J., and R. Nusse. 2004. Convergence of *wnt*, β-catenin, and cadherin pathways. *Science.* 303:1483–1487.
25. Huber, O., C. Bierkamp, and R. Kemler. 1996. Cadherins and catenins in development. *Curr. Opin. Cell Biol.* 8:685–691.
26. Jankowski, J. A., R. Bruton, N. Sheperd, D. Scott, and A. Sanders. 1997. Cadherin and catenin biology represent a global mechanism for epithelial cancer progression. *Clin. Pathol. Mol. Pathol.* 50:289–290.
27. Kemler, R., A. Hierholzer, B. Kanzler, S. Kuppig, K. Hansen, M. M. Taketo, W. N. de Vries, B. B. Knowles, and D. Solter. 2004. Stabilization of β-catenin in the mouse zygote leads to premature epithelial mesenchymal transition in the epiblast. *Development.* 131:5817–5824.
28. Jamora, C., R. DasGupta, P. Koclenlewski, and E. Fuchs. 2003. Links between signal transduction, transcription and adhesion in epithelial bud development. *Nature.* 422:317–322.
29. Shimamuram, K., and M. Takeichi. 1992. Local and transient expression of E-cadherin involved in mouse embryonic brain morphogenesis. *Development.* 116:1011–1019.
30. Chen, Y.-T., D. B. Stewart, and W. J. Nelson. 1999. Coupling assembly of the E-cadherin/β complex to efficient endoplasmic reticulum exit and basal-lateral membrane targeting of E-cadherin in polarized MDCK cells. *J. Cell Biol.* 144:687–699.
31. Lee, E., A. Salic, R. Kru, R. Heinrich, and M. W. Kirschner. 2003. The roles of APC and axin derived from experimental and theoretical analysis of the Wnt pathway. *PLoS Biol.* 1:116–132.
32. Seman, G. 2005. Propagation of breast cancer cells in aggregate cultures. *Meth. Cell Sci.* 6:3–4.
33. Mahaffy, R. E., C. K. Shih, F. C. McKintosh, and J. Kaes. 2000. Scanning probe-based frequency-dependent microrheology of polymer gels and biological cells. *Phys. Rev. Lett.* 85:880–883.
34. Alcaraz, J., L. Buscemi, M. Grabulosa, X. Trepat, B. Fabry, R. Farre, and D. Navajas. 2003. Microrheology of Human lung epithelial cells measured by atomic force. *Biophys. J.* 84:2071–2079.
35. Chesla, S. E., P. Selvaraj, and C. Zhu. 1998. Measuring two-dimensional receptor-ligand binding kinetics by micropipette. *Biophys. J.* 75:1553–1557.
36. Stevens, A. 2000. The derivation of chemotaxis equations a limit dynamics of moderately interacting stochastic many particles systems. *SIAM J. Appl. Math.* 61:183–212.